FEASIBILITY STUDY ON THE FUTURE IMPACT OF ELECTRIC VEHICLE FLEETS ON THE POWER SYSTEM INERTIA FLOOR

A Thesis

by

OLUWATOYIN OLADOTUN OSHINKOYA

Submitted to the Graduate and Professional School of
Texas A&M University
in partial fulfillment of the requirements for the degree of

MASTER OF SCIENCE

Chair of Committee,	Adam Birchfield
Committee Members,	Thomas Overbye
	Jeyavijayan Rajendran
	Astrid Layton
Head of Department,	Miroslav Begovic

May 2023

Major Subject: Electrical Engineering

ABSTRACT

The use of electric vehicle fleets such as clean school buses and readily available charged batteries in charging stations is proposed to participate in the frequency regulation of the grid when the support is needed, especially during a huge disturbance on the grid. As the nation moves into more cleaner generating resources which are added to the grid through inverter-based resources, the inertia of the power system is decreased. The goal is to reduce the floor of synchronous inertia necessary to maintain stable operation. To prove the concept, the synthetic Texas 7k bus case system with varying inertia values are used. The base case is assumed to have 100% inertia with 386GWs inertia capability. The dynamic model of this case is modified to vary the inertia to certain percentages of the base case inertia for comparison. The simulation results shows that the rate of change of frequency (RoCoF) and the frequency nadir at some inertia level reduces to a value below the Under-frequency load shedding (UFLS) threshold frequency when there is an N-2 generator contingency of 2558 MW generation loss on the system. However, with the implementation of the electric vehicle fleets through the Vehicle-to-grid application, the RoCoF and frequency nadir improves to a value higher than the UFLS threshold frequency under the same contingency of 2558 MW generation loss.

DEDICATION

I dedicate this thesis to my grandparents, my parents and my family for their support and encouragement.

ACKNOWLEDGMENTS

First and foremost, I would like to thank my advisor, Dr. Adam Birchfield for giving me the opportunity to conduct my Masters thesis under his supervision and guidance. His advises has been a source of encouragement and motivation throughout the course of my research. His weekly group meetings were significant for my learning and development as a research student in the Energy and Power Group. I would also like to thank Dr. Thomas Overbye, Dr. Jeyavijayan Rajendran and Dr. Astrid Layton for serving on my committee.

As a graduate student, I was fortunate to take Dr. Birchfield's and Dr. Overbye's classes on Power System Stability, Analysis, and Transients. I have learned a lot from their classes, and I can say that I am a better student because of the knowledge they have impacted. I would like to thank the department faculty and staff of Texas A&M University Graduate and Professional School for making my time here at Texas A&M a great experience.

I would also like to thank all my fellow research group members in Dr. Birchfield's research group, but especially Jong-oh Baek who built the cases used for my studies. Rida Fatima for her constant words of encouragement. I am also thankful for the opportunity to work with Dr. Thomas Overbye's group on some research projects related to Electric Vehicles.

Finally, I would like to thank my family for their constant support and encouragement that keeps me going. Words can never fully express my gratitude.

CONTRIBUTORS AND FUNDING SOURCES

This work was supported by a thesis committee consisting of adviser Prof. Adam Birchfield, Prof. Thomas Overbye, Prof. and Prof. Jeyavijayan Rajendran, of the Department of Electrical and Computer Engineering, and Prof. Astrid Layton of the Department of Mechanical Engineering. The cases used were provided by Prof. Birchfield and Jong-oh Baek of the Department of Electrical and Computer Engineering. All other work conducted for the thesis was completed by the student independently.

Graduate study was partly supported by the Thomas W. Powell '62 and Powell Industries Inc. Fellowship from the Department of Electrical and Computer Engineering at Texas A&M University.

NOMENCLATURE

AGC	automatic generation control
BESS	battery energy storage system
EMS	Energy Management System
ERCOT	Electric Reliability Council of Texas
EV	electric vehicle
FO	fleet operator
QSGR	Quick Start Generation Resources
GW	gigawatt
GWs	gigawatt-second
Hz	Hertz
IR	inertia response
kW	kilowatt
MW	megawatt
MW	megawatt-second
NLM	Negative Load Model
RoCoF	rate of change of frequency
SC	synchronous condenser
SG	synchronous generators
UC	ultracapacitor
UFLS	underfrequency load shedding
U.S.	United States
V2G	vehicle-to-grid

WECC	U.S. Western Electricity Coordinating Council

TABLE OF CONTENTS

Page

LIST OF FIGURES

FIGURE Page

LIST OF TABLES

TABLE Page

1. INTRODUCTION AND LITERATURE REVIEW

1.1 Introduction

The modern power system generates electricity using various power generating sources. According to the U.S. Energy Information Administration (EIA), natural gas, nuclear energy, and coal generated most of the nation's electricity in 2020 [6]. Renewable resources like wind, solar, hydro-power, geothermal, and biomass have been implemented in the generation of electricity for the purpose of decarbonizing the electrical grid. These resources generated 20% of the nation's electricity in 2020 [6]. These renewable resources are projected to supply 44% of electricity generation by 2050 [7]. The increasing penetration of renewable power generation on the grid decreases the inertia capability of the grid.

Power system inertia is the ability of the power system to resist the drop in frequency after a generator failure by supplying the kinetic energy stored in the rotating mass of the generators to keep the whole system running before other frequency response devices respond to the change in frequency. The inertia response is typically available for a few seconds to support the grid in maintaining the frequency to prevent the tripping of under-frequency relays.

Frequency is controlled by the ability of the power system to balance the system generation and demand. The nominal steady state system frequency of the North American power system is 60 Hz. A significant imbalance of the system leads to a large deviation of the system frequency. The ability of the power system to maintain the nominal frequency of 60 Hz during normal conditions and to recover the frequency change after imbalance conditions is referred to as the frequency stability [8]. The first stage to stabilize the system frequency is the inertia response (IR), which is the release of the stored kinetic energy in the synchronous generators. This is followed by the primary frequency reserve (PFR) which stabilizes the frequency to a value close to its nominal value with an allowed error. The secondary frequency reserve (SFR) relieves the PFR, and the

tertiary frequency reserve (TFR) provides support by rescheduling the previous generation [9]. Figure 1.1 below shows the frequency response of a system, with the inertia response typically at time 0-10s. The scope of this work is to focus on the inertia response (IR).

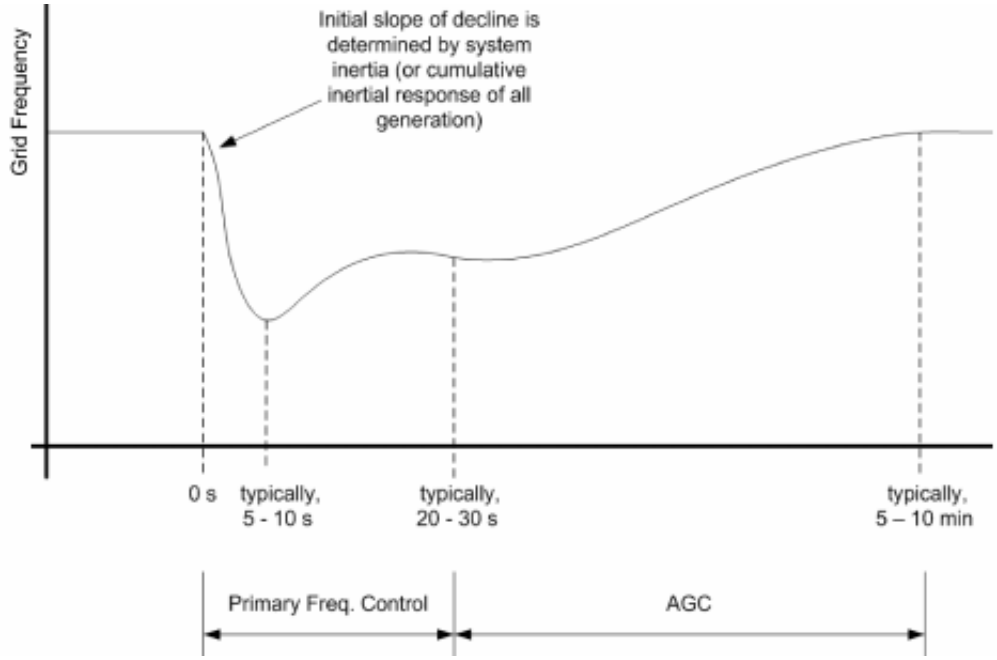

Figure 1.1: Inertial, primary frequency controls, and AGC (secondary) response. Reprinted from [1].

The electrification of vehicles is the current trend in the development of vehicles. Not only has it become a solution for the environment, but it is also an energy storage system for buffering the grid power. Most electric Vehicles (EVs) fleets are parked more than 20 hours each day, making them ideal to store excess power from the grid and send back during peak hours [10]. The purpose of these EV fleets is to utilize their ability to provide ancillary service to the transmission system operators and automatic generation control based on their spinning reserve services benefits, regulation, ramp-up, and ramp-down applications. These services are accomplished through optimal charging of the EV station such as charging during non-peak load hours, minimization of voltage drops, and holding up to 50% of excess wind energy. These services will be controlled

by an electrical fleet operator (FO). The roles of these electrical fleet operators are to ensure the vehicles owners' needs, provide needed ancillary services and utilize V2G applications to provide peak power. When providing ancillary services, the system's operator needs to maintain the supply and demand between the grid and fleet's battery bank. Automatic Generation Control has to coordinate to respond within a minute for proper spinning reserve restoration along with up and down regulation back to the required frequency. Ancillary services also go beyond the grid by supporting the distribution of power to the electrical vehicles themselves. Smart charging can control the charging rate of EVs to help avoid voltage limitations and congestion along the power grid. Finally, additional services include more renewable energy integration and its applications as a storage device [11].

Therefore, this paper studies the potential benefits of Vehicle-to-grid (V2G) technology for inertia frequency regulation. This paper presents a study from the Texas 7k bus case with different inertia values to represent the modern power grid. The impact of these various inertia levels on the frequency response of the grid after a sudden disturbance is studied and presented.

The rest of this paper is organized as follows: Section II examines the power system inertia and introduces the different techniques proposed in other papers for a low inertia power system. Section III demonstrates a collection of case studies based on the Texas 7k bus case with varying inertia values. Section IV provides discussions on the proposed technology for inertia enhancement. Conclusions and future works are discussed in Section V.

1.2 Background

The power system consists of hundreds or thousands of synchronously connected generators at a grid frequency of 60 Hertz (Hz) in the U.S. These synchronous generators store kinetic energy that will be automatically extracted following a sudden loss of generation. The extraction of the stored kinetic energy causes the generators to slow down, inherently, causing the frequency of the system to decay. The frequency of the system reflects the health of the grid as it pertains to its ability to balance supply and demand [8]. Therefore, the reliability of the power system is dependent on the inertia of the system.

As renewable sources penetration through inverter-based resources increases in the power system, the number of synchronous generators decreases. Consequently, the power system inertia decreases because of its direct relationship to the number of synchronous generator in the system. As the inertia decreases, the Rate of Change of Frequency (RoCoF) and the frequency nadir of the system increases after a disturbance. This may result in involuntary load disconnection if the RoCoF is high enough that there is no sufficient time for other mechanisms to resist the frequency decay from dropping below the system's under-frequency load shed set points [2].

The inertia of a system is a feature of the synchronous generators (SG) present in the system. Therefore, the amount of inertia is dependent on the number of on-line generators. The inertia constant is expressed as H, and the total inertia of the system is defined by [12] and modified as:

$$H_{total} = \sum_{i=1}^{n} H_i S_{sys} \tag{1.1}$$

where H_i is the inertia constant for an i^{th} online SG, and S_{sys} is the MVA rating of the system. Table 1.1 shows the ranges of inertia constant, and Inertia response contribution based on resource type as defined by the Energy Reliability Council of Texas (ERCOT). It is shown that Wind and Solar PV have no inertia response contribution to the grid because they are inverter-based resources and are connected to the grid without rotating mass, which is responsible for inertia.

Table 1.1: Inertia constant and Inertia response contribution by Resource Type. Adapted from [2]

Resource Type	**H(s)**	**H*MVA base (MWs)**
Nuclear	3.8-4.34	5344-6530
Coal	2.9-4.5	863-3158
Combustion Turbine	1-12.5	22-1288
Gas Steam	1-5.4	13-2216
Combined Cycle	1.1-9	97-8765
Hydro	2-3	19-1133
Reciprocating Engine	1.1-2.1	13-97
Wind	0	0
Solar PV	0	0

The hour of day and season of the year impacts the number of online synchronous generator on the system. As shown in Figure 1.2 the impact of season of the year on the inertia capability of the system in the year 2017. There are fluctuations in the system inertia values showing the general trend that the system inertia is highest during the summer and lowest during the shoulder months. This is as a result of more online synchronous generators in the system to serve the higher load in the summer. The synchronous generation commitment is highly affected by the load and the amount of non-synchronous generation like renewable resources on the system. For economic reasons, if the amount of wind and solar generation is abundant during low load conditions, the synchronous generators remain offline. This will consequently reduce the system inertia. Figure 1.3 shows the hourly inertia conditions for 2015, 2016, and 2017 and their corresponding wind penetration. The different units on the system have different commitment constraints which affects the total system inertia [2].

ERCOT implemented a network-model-driven inertia calculation into their EMS system in 2017. This model tracks the online status of the Private Use Network Resources and the net output to identify the online status of all the other resources. The unit is considered online if the net output of the Resource is above 5MW. Then the inertia constant of each online unit in seconds is multiplied by their corresponding MVA base to calculate the inertia contribution of each online unit. Presently, the synchronous inertia which is calculated in EMS is also monitored in Real-Time using three-level-based visual alarming approach to ensure situational awareness. The Control Room will closely monitor the grid conditions in the event that the inertia drops below the 120GWs threshold. When the inertia drops below 105GWs, the operators will take appropriate actions for the restoration of the inertia to a level at or above 105GWs. There are several potential actions that may be employed to mitigate the situation, including the deployment of Non-Spin from the Offline Generation Resources, the commitment of the remaining Quick Start Generation Resources (QSGR) that are not responsible for Non-Spin, and lastly, by committing the Generation Resources that can be started within an hour [2].

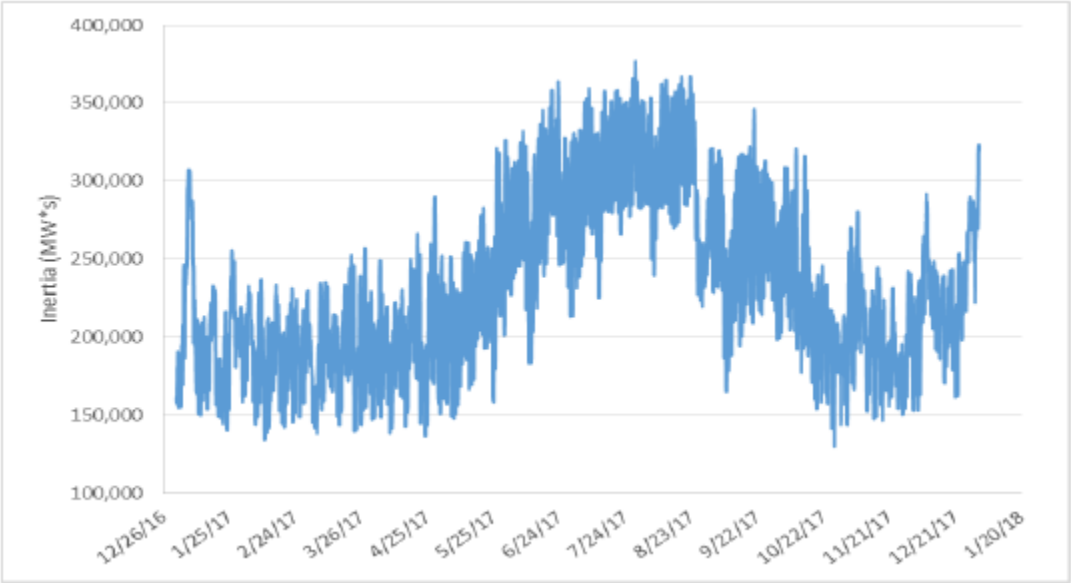

Figure 1.2: Inertia in 2017 to depict the impact of hour of day and season of the year on system inertia. Reprinted from [2].

1.3 Proposed Technology

The relationship between the SG and inertia raises a system stability concern for the grid operators as the penetration level of renewable sources increases. Many control methods have been studied to alleviate the low inertia issue of the system. References [13] and [14] explores the contribution of synchronous condenser (SC) to frequency stability enhancement. The retired SGs are proposed to be converted to SCs for additional inertia to improve frequency response performance. The results of the studies in these papers supported the notion that SCs can improve the network frequency response. However, this operation will impose some costs on the operators. Ultracapacitor (UC) is proposed in [15] because of their fast response capabilities similar to batteries. The results of the studies in this paper concluded that the frequency response of an ideal model is the same as that of a nonlinear model. However, there are different models with different capacitance values which will discharge at different rate. This may make the ideal representation of the realistic behavior inadequate if the energy requested is bigger than the stored energy in the ultracapacitor, leading to an erroneous conclusion about the frequency response. [16] introduces the implementa-

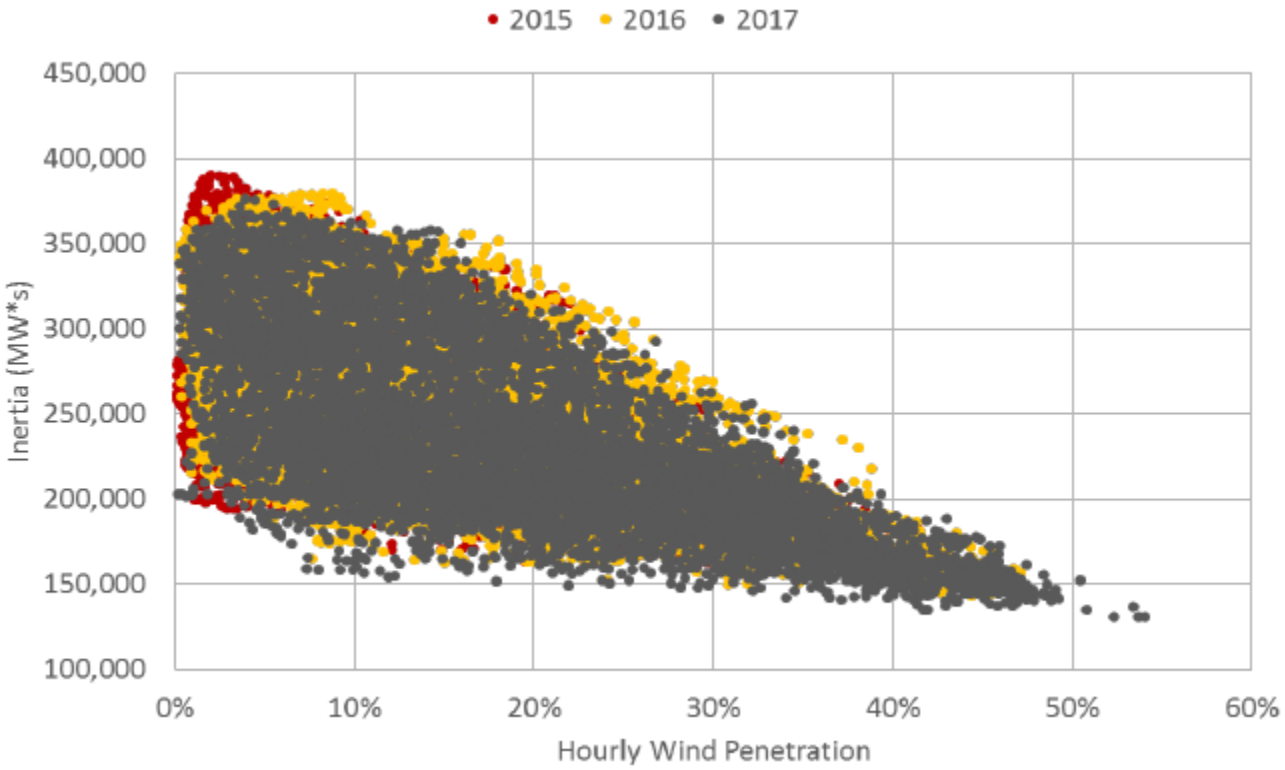

Figure 1.3: The correlation between Inertia and Wind Penetration in 2015, 2016, and 2017. Reprinted from [2].

tion of a synthetic grid control mechanism for a wind generator. This control mechanism emulates the inertia response of a traditional generator by exploiting the energy content provided by the capacitor of a suitably sized DC link. This method was tested on a small scale network and a portion of the Italian power system to corroborate its effectiveness. The results showed that the synthetic inertia was able to enhance the frequency stability of the system after an under-frequency event. Some improvements to increase the performance of the system are encouraged.

The V2G technology has gained a lot of attention because of the advance in battery technologies and the promise of a clean and efficient transportation. Several federal incentives has been put in place to promote the electrification of transportation [17]. By 2030, the EVs on U.S. roads have been projected to reach 26.4 million [18] . V2G is proposed in [19] to solve the problem of load and demand imbalance by using the large amount of stored energy in EVs as a buffer for the power grid and renewable energies. [20] explained the feasibility of V2G realization by using the EVs

batteries. Different categories of this realization to provide reasonable energy from the EVs to the grid based on the grid requirement are also explained. V2G is still a relatively new technology and more research in this area is encouraged to study the application.

2. PROPOSED ANALYSIS METHODOLOGY FOR EV IMPACTS ON FREQUENCY RESPONSE

2.1 Electrical Vehicle Fleets

When modeling the inertia cases, the concept of Electrical Vehicle fleets as a Battery Energy Storage System (BESS) can be used by utilizing the approved U.S. Western Electricity Council (WECC) models for power system stability analysis. These models have been configured, parameterized, and tuned in power system simulation software platforms to be used for representing the steady state and dynamic performance of BESS. Figure 2.1 shows an overview of the three WECC generic model modules used for grid frequency regulation and voltage support. The battery energy storage control module (REEC_C) needs to interact with two other system models (REGC_A and REPC_A) to represent the BESS for frequency regulation at transmission level [3]. These models are more attractive for future studies because of their generic and flexible nature.

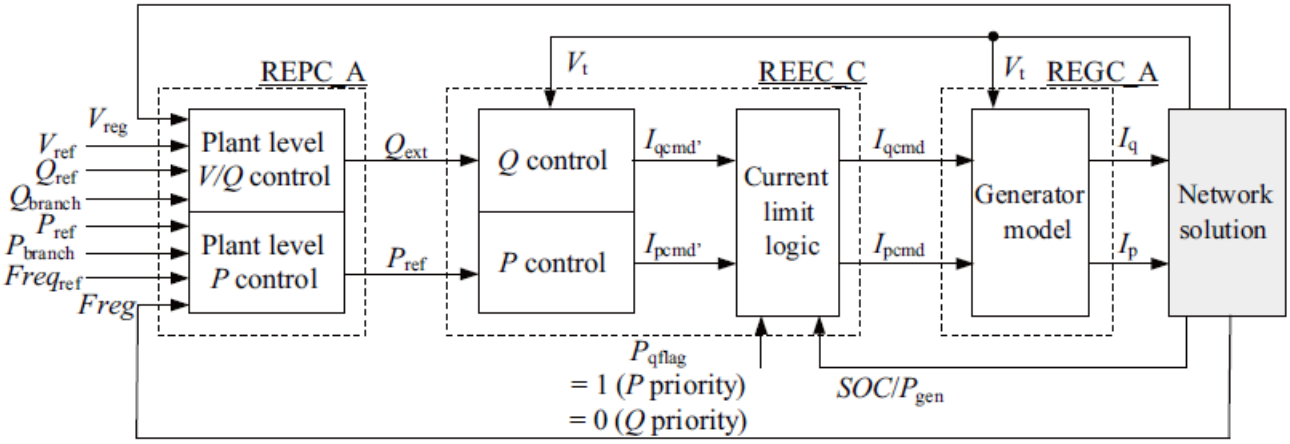

Figure 2.1: Overall model structure using the WECC generic model. Reprinted from [3].

* ©2023 IEEE. Reprinted with, permission from, O. Oshinkoya, J. -O. Baek, J. Kao and A. Birchfield, "Preliminary Analysis of the Potential Impact of Electric Vehicle Fleets on Large Power System Inertia Floor," *2023 IEEE Texas Power and Energy Conference (TPEC)*, March 2023.

The CBEST battery model can also be utilized for modeling these EVs fleets on the power system. However, other work [3] has pointed out that this model was developed for specific battery storage projects and has some limitations in the plant controls and state-of-charge logic models [3].

For power flow analysis, EVs can be modeled as a machine connected to the grid. The EV discharging and charging conditions can be represented as positive generation or negative generation of the machine's MW output. This can be used in modeling the machine capability to regulate the frequency when the frequency drops to a certain threshold.

Recent analysis showed that a generation loss of 2750 MW on a low system inertia would cause the frequency to decline from 59.7 Hz to 59.3 in 0.416 seconds [2]. Therefore, the response time of the EVs fleet for grid support should be less than 0.416 seconds to arrest the frequency decay. According to [21], the average EV capacity is 40kW. For a generation loss of 2750 MW, 68,750 EVs will be required to support the grid. It should be noted that there are 791,384 EVs on Texas roads today, and a cumulative charging ports of 126,017 [22]. Additionally, EV fleets are being explored by the US government. Currently there are 2,352 electrical school buses in the US, but the push for additional electrical school buses, the clean school bus program, is being pushed by the US government with the Biden Administration providing rebate awards totaling 1 Billion US dollars. With the addition of the EV school buses it is more than likely more large charging stations and their corresponding fleets will appear across the US with the ability to provide ancillary services [23].

2.2 Negative Load Modelling

In a normal system state with the incorporation of EVs, there is a power consumption of some certain MW value at an EV's charging station. This is regarded as a Positive Load on the system bus. For a contingency system state, there is a power transfer from the EVs to the grid. This is regarded as a Negative Load on the system bus. These two loads are added to a bus to represent the normal and contingency state. The Electric Vehicle Fleets is modeled as a Negative Load on the system for frequency stability studies. To depict a normal operation, the demand from the EV charging station is aggregated to the buses in the power grid simulation as a positive load at that bus.

Whereas for the contingency operation, the supply from the EV charging station is aggregated as a negative load at that bus. Figure 2.2 shows the overall structure of the model. It is shown that the negative load which is a negative active power is injected into the bus. This will aid the regulation of the system frequency when there is a generation outage by keeping the frequency from dropping below a certain threshold to avoid tripping of generators and eventually load shedding.

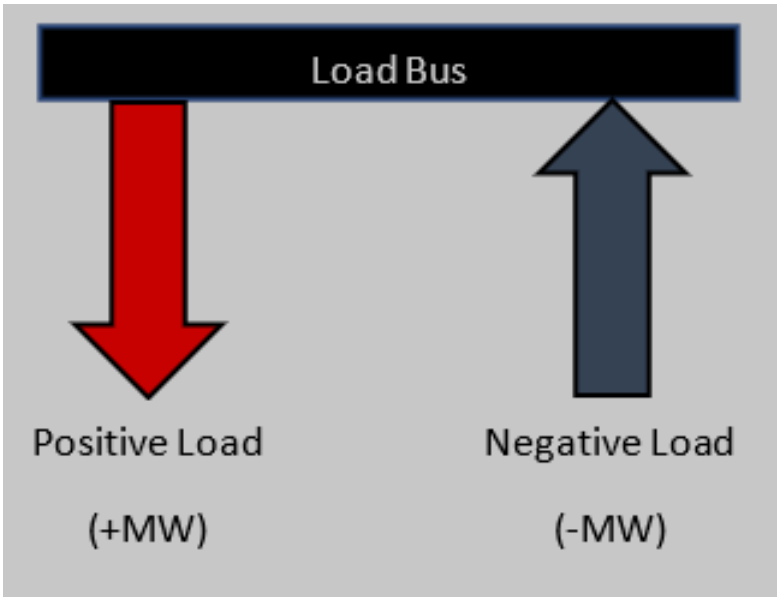

Figure 2.2: Overall model structure of the Negative Load modeling.

3. POWER SYSTEM CASE STUDY

3.1 Case Study

This paper uses the Texas 7k bus synthetic grid case [24] as shown in Figure 3.1 as the studied network. This simulation system is a fictitious network geographically located in Texas. It does not represent the real grid and is publicly available online [25]. The attributes of the case are highlighted in Table 3.1. The system frequency is observed at various inertia levels during a N-2 contingency study.

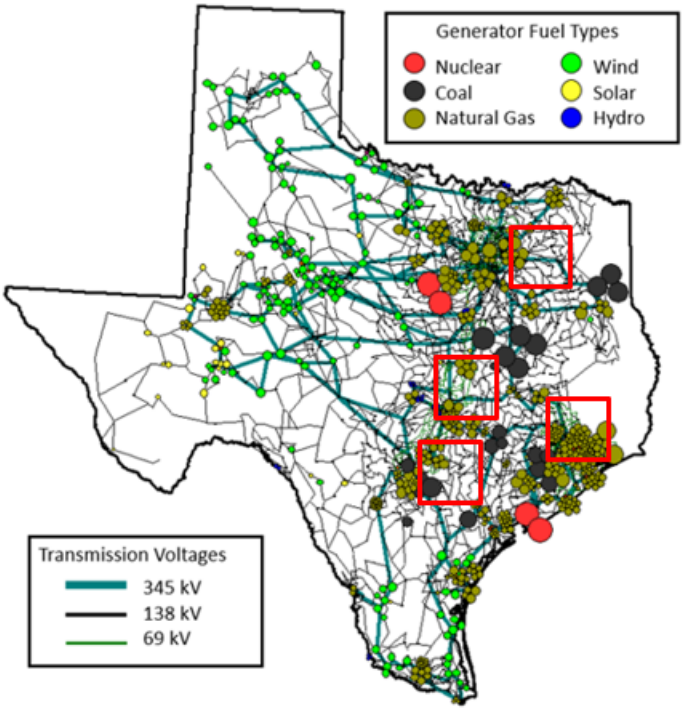

Figure 3.1: Texas 7K Bus Synthetic Case.

* ©2023 IEEE. Reprinted with, permission from, O. Oshinkoya, J. -O. Baek, J. Kao and A. Birchfield, "Preliminary Analysis of the Potential Impact of Electric Vehicle Fleets on Large Power System Inertia Floor," *2023 IEEE Texas Power and Energy Conference (TPEC)*, March 2023.

Table 3.1: Texas Synthetic Bus Case Information

Parameter	Value
Buses	6717
Generators	731
Loads	5095
Switched Shunts	634
Areas	8
Substations	4894
Transmission Lines	7173
Total Generation (MW)	77546.5
Total Load (MW)	74666.5

3.1.1 Simulation

For the purpose of this study, the case study is simulated using PowerWorld simulator. PowerWorld simulator is a widely known software utilized by power industries in North America and other countries.

Twelve separate cases were developed from the Texas 7k bus synthetic grid case to study the behavior of the power system at different levels of inertia. The synthetic case which is available online [25] was altered by a PhD student, Jong-oh Baek under the supervision of Dr. Adam Birchfield. These cases were modified by decommitting synchronous generators to reflect the current trend in the power system as more inverter-based renewable resources are added to the grid for the purpose of decarbonizing the grid. As a result, the generation were also varied. The purpose of this modification is to study the effect of different inertia levels on the power system frequency response and also to run the desired studies to study the impact of EV fleets for providing inertia support to the power system.

There are four nuclear power plants with a total capacity of 4958 MW. However, only two of the nuclear power plants are considered in this study. The two biggest nuclear units generating 2558 MW are outaged to study the frequency response of the system under varying inertia values as shown in Table 3.2. The frequency nadir and the RoCoF are the metrics used for determining the frequency response of the system. Frequency nadir shows the lowest frequency after a disturbance.

RoCoF represents how fast frequency changes after a sudden imbalance between generation and load occurs [26]. RoCoF is given in [26] as:

$$RoCoF_T = \frac{|f_T - f_0|}{T} \tag{3.1}$$

where $RoCoF_T$ is the difference between the two frequency measured divided by the calculated window of time, expressed as Hz/s [26].

The goal is to maintain a low RoCoF because a high enough RoCoF could lead to three major issues explained in [27], such as:

- Unintentional tripping as a result of inaccurate frequency and/or RoCoF measurement.
- Over extensive load shedding when the frequency falls below a certain threshold corresponding to a percent of the total load while shedding a much less percent of the load.
- Frequency collapse before there is time for the relays to trip.

Table 3.2: Varying Inertia Case Information. Reprinted from [4]

Case (#)	**Generation (MW)**	**Wind Gen. (%)**	**Inertia Value (GWs)**
1	77547	27.9	386.5
2	53659	26.4	315.1
3	54053	33.2	241.3
4	34237	22.7	228.3
5	34252	25.8	211.9
6	34289	26.9	195.4
7	34331	23.2	179.8
8	34381	24.6	163.9
9	34458	25.6	146.8
10	34483	27.4	131.8
11	30585	26.9	116.3
12	26666	27.2	100.8

3.1.2 Results and Discussions

This section presents the results for the contingencies with relevant discussions. In the simulated scenarios of these simulation studies, the impact of a sudden generation change on the system is studied. The base case inertia is calculated to be 386.504 GWs. To vary the inertia of the system, some generators are decommitted, thereby varying the generation. This is shown in Table 3.2. For contingency analysis, the two largest nuclear generators responsible for a total generation of 2558 MW are outaged at time = 1s, leaving an imbalance in the generation and load of the system.

Figure 3.2 shows the simulated results for frequency response at different inertia values over the range of 10 seconds as that is the typical inertia response time. It can be seen that the decrease in inertia deteriorates the frequency response of the system. Table 3.4 shows the values of the frequency nadir corresponding to each inertia case. Whereas, Table 3.5 shows the rate at which the frequency changes according to each inertia case. In Figure 3.3, the frequency nadir and the under-frequency load shedding (UFLS) threshold are depicted.

Under-frequency load shedding (UFLS) is a protection scheme set in place to protect the power system by stabilizing the balance between load and generation. This scheme is employed when the system frequency falls below a specified value [28]. Table 3.3 shows the set points for the UFLS [29]. The table shows a load shed of 5% for a frequency of 59.3 Hz, an additional 10% load shed for 58.9 Hz, and an additional 10% load shed for 58.5 Hz.

Figure 3.3 shows the inertia cases 11 and 12 to have a minimum frequency less than the UFLS set point of 59.3 Hz. As explained in Table 3.3, this will trip the shedding of 5% of the total load on the system to balance the demand and supply. These two cases are most important to the future studies of this paper. The goal is to use Electric Vehicle fleets to provide inertia responses in cases like 11 and 12 where the inertia of the system is less than the required inertia needed to support the system, resulting in a threshold frequency that leaves the system vulnerable to involuntary load shedding. It is however important to note that the Inertia floor identified by ERCOT is 100 GWs [2]. The lowest inertia experienced by ERCOT to date is 116 GWs in 2021 where the inertia was lower than 120 GWs for 15 hours [30].

Table 3.3: Texas Under-frequency Load Shedding (UFLS) Set Points

UFLS Step	Frequency (Hz)	Load Shed (%)
1	59.3	5
2	58.9	10
3	58.5	10

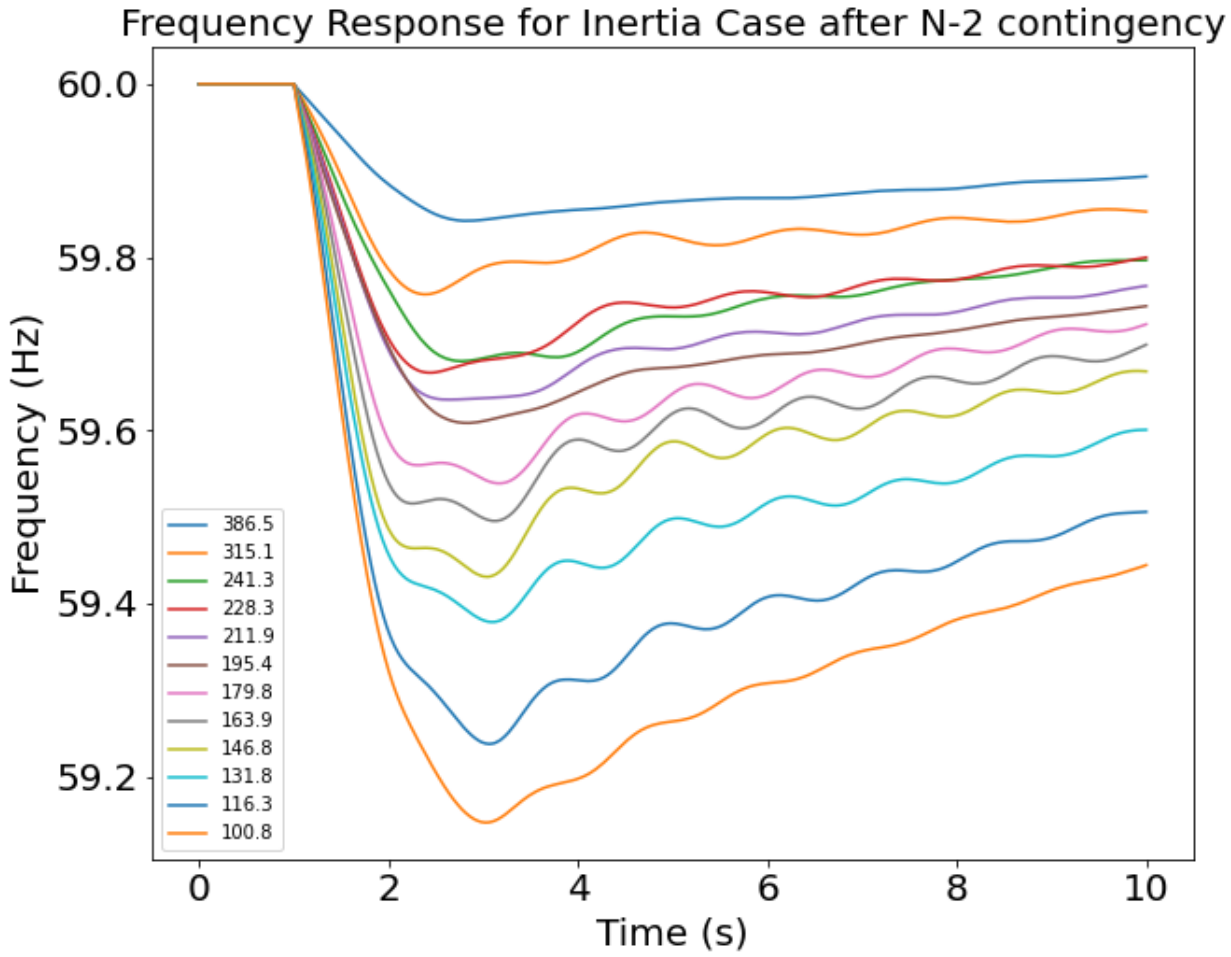

Figure 3.2: Frequency Response after 2558MW Generation loss with the different color corresponding to the Inertia value in GWs as shown in the legend.

Table 3.4: Frequency Nadir for Inertia Cases

Case (#)	System Inertia (GWs)	Frequency Nadir (Hz)
1	386.5	59.84
2	315.1	59.76
3	241.3	59.68
4	228.3	59.67
5	211.9	59.64
6	195.4	59.61
7	179.8	59.54
8	163.9	59.49
9	146.8	59.43
10	131.8	59.38
11	116.3	59.24
12	100.8	59.15

Table 3.5: RoCoF for Inertia Cases

Case (#)	System Inertia (GWs)	RoCoF (Hz/s)
1	386.5	0.06
2	315.1	0.10
3	241.3	0.13
4	228.3	0.13
5	211.9	0.13
6	195.4	0.14
7	179.8	0.15
8	163.9	0.16
9	146.8	0.19
10	131.8	0.20
11	116.3	0.25
12	100.8	0.28

3.2 Negative Load Model Simulation

The Negative Load model is implemented into the inertia case studies for studying the effect of the EV Fleets on the system frequency. The positive and negative load as explained in the modeling section are added to the bus for the normal and contingency operation. The buses at four large cities in Texas —Austin, Dallas, Houston, and San Antonio —are considered for these

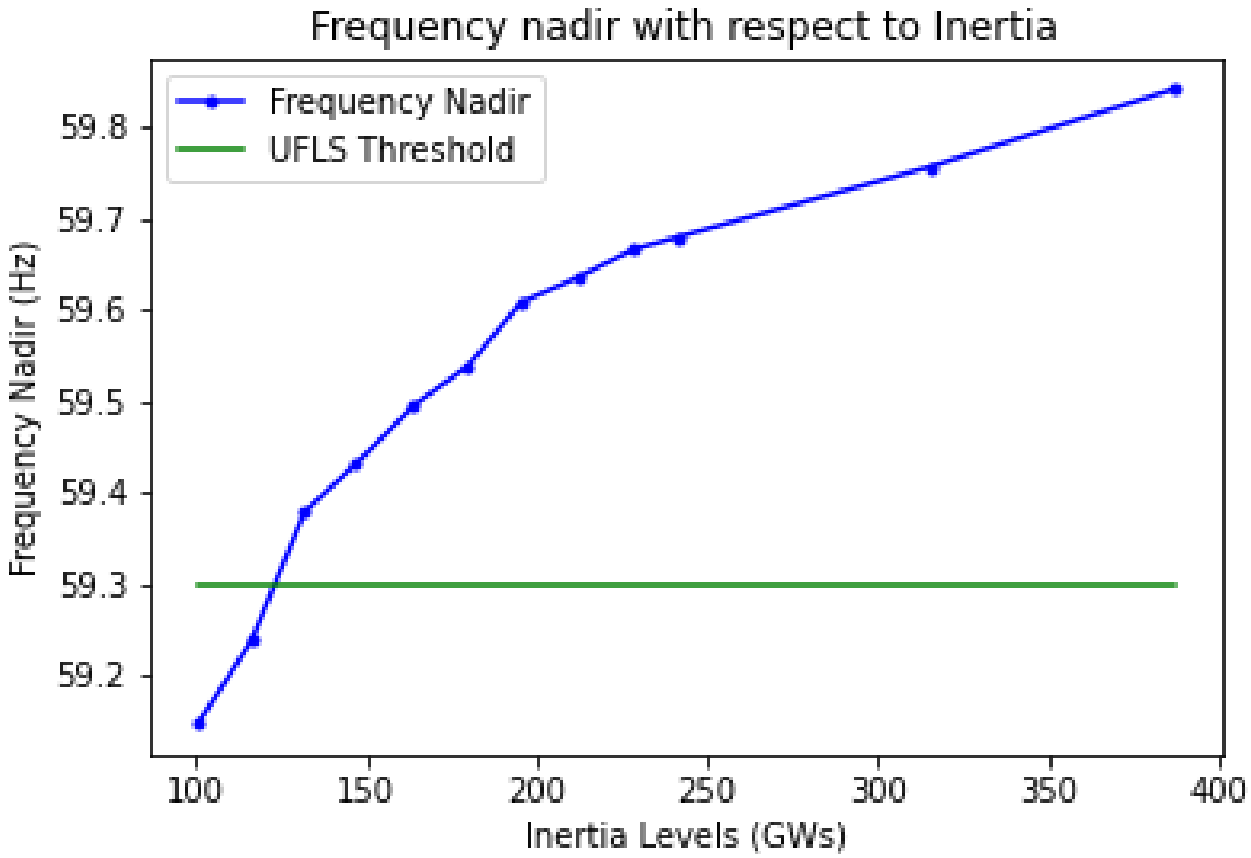

Figure 3.3: Frequency Nadir for different system inertia. Reprinted from [4].

studies. The assumptions made based on available information are:

- Individual Charging station has 20 charging ports.
- 50 and 100 charging ports are assumed for future integration of Electric Vehicles.
- Power per port is dependent on the charger level with Level 1 being 1kW and Level 2 being 7kW.
- Charging rate is the same as discharging rate.
- Each bus has a load calculated using number of ports, power per port (P_i), and number of charging stations in each city as shown in Table 3.6. The positive load is calculated using

the equation as shown below as:

$$Load_{+ve} = \#_{chargingstation} \sum_{i=1}^{20} P_i \tag{3.2}$$

- The negative load is the negative of the positive load. The negative load is calculated using the equation as shown below as:

$$Load_{-ve} = (-)\#_{chargingstation} \sum_{i=1}^{20} P_i \tag{3.3}$$

With the above assumptions and Table 3.6 information, the positive and the negative loads for the load bus in each city is calculated. An example of hw the information is added on the load bus is shown in Figure 3.4. The positive load is initially closed and the negative load is initially open to reflect a normal operation. These calculated values are added to the case information on PowerWorld to run the studies. For the transient simulation, the positive load is opened and the negative load is closed to show the change in power flow.

Table 3.6: EV Charging Station in Texas. Adapted from [5]

City	**Total # of Charging Stations**
Austin	893
Dallas	364
Houston	549
San Antonio	232

3.3 Results and Discussions

This section presents the results for the Negative Load contingencies with relevant discussions on the comparison of the case with and without the NLM. In the simulated scenarios of these simulation studies, the impact of EV Fleets on inertia response after a sudden generation change on the system is studied for cases 10 through 12. The calculated power capacity for the inertia

Location	Houston		Dallas		Austin		San Antonio	
Bus #	110802		130287		140079		120342	
Name of Bus	Houston 37 2		Dallas 37 2		Austin 16 2		San Antonio 37 1	
ID #	EV	3	EV	2	EV	2	EV	2
MW Value	10.98	-10.98	7.28	-7.28	17.86	-17.86	4.64	-4.64
Status	Closed	Open	Closed	Open	Closed	Open	Closed	Open

Figure 3.4: Load Bus information for the Texas Cities.

response from the EV fleets is shown in Figure 3.4. For the overall transient stability contingency analysis of the study, the two largest nuclear generators responsible for a total generation of 2558 MW are outaged at time = 1s, the positive load are opened at time = 1.5s, and the negative load are closed at the same time of 1.5s to give the system enough time to respond to the changes.

Figure 3.5–3.10 shows the simulated results for frequency response at 131GWs (case 10) inertia value with their MW support over the range of 10 seconds for the base case, base case with the positive EV load only, and base case with the NLM implemented. It can be seen that with just the positive EV load on the base case, the frequency nadir drops further. The implementation of the NLM helped improve the frequency response. Table 3.7 shows the values of the frequency nadir corresponding to Case 10 base case, base case with positive EV load and base case with the NLM for different charging levels and ports. Case 10 from the base case has the frequency nadir of value 59.38Hz and this drops further with the positive EV load added, but with the inclusion of the EV fleets using the NLM, we can see that the frequency improved to 59.63Hz. This supports the conclusions arrived from the figures.

Figure 3.11–3.16 shows the simulated results for frequency response at 116GWs (case 11) inertia value with their MW support over the range of 10 seconds for the base case, base case with the positive EV load only, and base case with the NLM implemented. It can be seen that with just the positive EV load on the base case, the frequency nadir drops further. The implementation of the NLM helped improve the frequency response. Table 3.8 shows the values of the frequency

nadir corresponding to Case 11 base case, base case with positive EV load and base case with the NLM for different charging levels and ports. Case 11 from the base case has the frequency nadir of value 59.24Hz and this drops further with the positive EV load added, but with the inclusion of the EV fleets using the NLM, we can see that the frequency improved to 59.40Hz. This supports the conclusions arrived from the figures.

Figure 3.17–3.22 shows the simulated results for frequency response at 100GWs (case 12) inertia value with their MW support over the range of 10 seconds for the base case, base case with the positive EV load only, and base case with the NLM implemented. It can be seen that with just the positive EV load on the base case, the frequency nadir drops further. The implementation of the NLM helped improve the frequency response. Table 3.9 shows the values of the frequency nadir corresponding to Case 12 base case, base case with positive EV load and base case with the NLM for different charging levels and ports. Case 12 from the base case has the frequency nadir of value 59.15Hz and this drops further with the positive EV load added, but with the inclusion of the EV fleets using the NLM, we can see that the frequency improved to 59.61Hz. This supports the conclusions arrived from the figures

Under-frequency load shedding (UFLS) as mentioned earlier is a protection scheme set in place to protect the power system. This scheme is activated when the system frequency drops below the specified frequency as shown in Table 3.3. The base case shows the inertia cases 11 and 12 to have a minimum frequency that is less than the UFLS set point of 59.3Hz. This will result in a load shed of 5% on the system as explained in Table 3.3. In Figure 3.23, the frequency nadir for the base case, the base case with the inclusion of the positive EV load only, the base case with the inclusion of NLM and the under-frequency load shedding (UFLS) threshold are depicted. With the inclusion of EV fleets as just a positive load, it is shown that the frequency nadir drops further in the cases they were implemented on. With the utilization of the NLM, it is shown that the minimum frequency of the cases 11 and 12 still falls below the UFLS first set point of 59.3Hz when the Level 1 charger is used. Although, there is an improvement from the frequency nadir achieved when only the positive load was added.

Figure 3.24 shows the comparison of the base case, base case with the positive EV load only, base case with the NLM, and the under-frequency load shedding threshold for the Level 2 charger. It is evident that the cases with the positive EV loads leads to a threshold frequency that makes the system extremely vulnerable. However, when the NLM was implemented, we see an improvement in the frequency, especially with the cases where 50 and 100 ports are used. The goal of this study is to use Electric Vehicle fleets to provide inertia responses in cases like 11 and 12 where the inertia of the system is less than the required inertia needed to support the system, resulting in a threshold frequency that leaves the system vulnerable to involuntary load shedding. It can be seen that the results of the study as shown in the figures and table achieved the intended goal set out to be achieved.

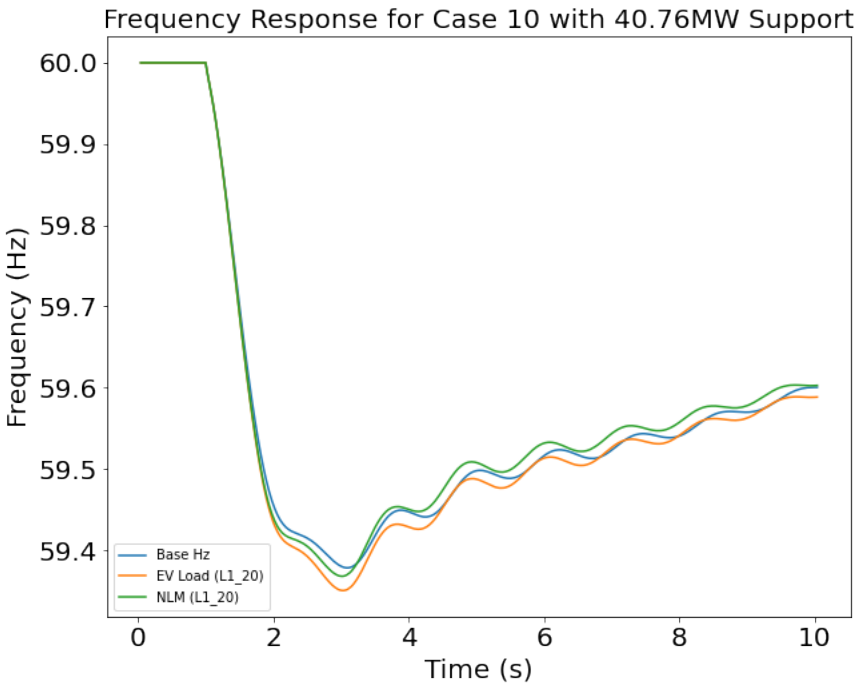

Figure 3.5: Comparison of Frequency Response using the 20 ports Level 1 charger of 1kW support per port on the base case, base case with just the positive EV load, and the base case with the Negative Load Model (NLM) on Case 10 with 131GWs.

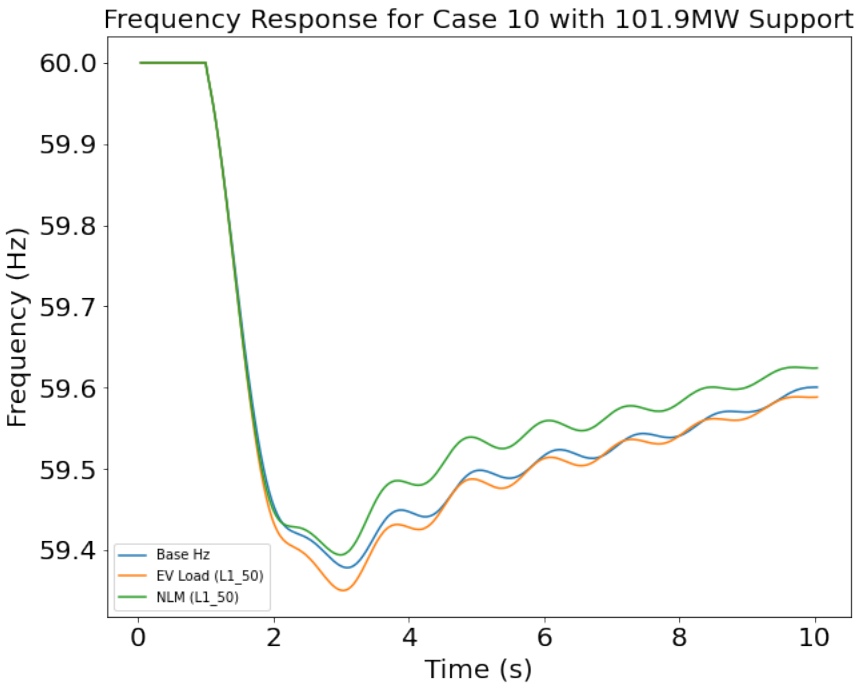

Figure 3.6: Comparison of Frequency Response using the 50 ports Level 1 charger of 1kW support per port on the base case, base case with just the positive EV load, and the base case with the Negative Load Model (NLM) on Case 10 with 131GWs.

Table 3.7: Frequency Nadir for Case 10 base case with and without NLM

Charger	**Charging Ports**	**Freq Nadir with EV load (Hz)**	**Freq Nadir with NLM (Hz)**
Level 1	20	59.35	59.37
Level 1	50	59.35	59.39
Level 1	100	59.35	59.44
Level 2	20	59.35	59.47
Level 2	50	59.35	59.54
Level 2	100	59.33	59.63

Table 3.8: Frequency Nadir for Case 11 base case with and without NLM

Charger	**Charging Ports**	**Freq Nadir with EV load (Hz)**	**Freq Nadir with NLM (Hz)**
Level 1	20	59.00	59.11
Level 1	50	59.00	59.14
Level 1	100	59.00	59.19
Level 2	20	59.00	59.23
Level 2	50	59.00	59.36
Level 2	100	58.98	59.40

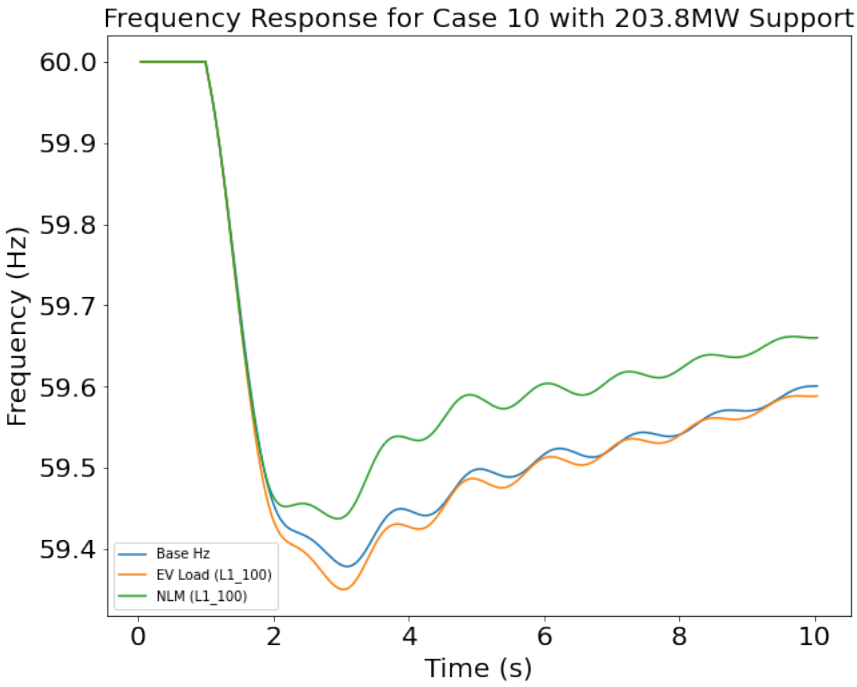

Figure 3.7: Comparison of Frequency Response using the 100 ports Level 1 charger of 1kW support per port on the base case, base case with just the positive EV load, and the base case with the Negative Load Model (NLM) on Case 10 with 131GWs.

Table 3.9: Frequency Nadir for Case 12 base case with and without NLM

Charger	**Charging Ports**	**Freq Nadir with EV load (Hz)**	**Freq Nadir with NLM (Hz)**
Level 1	20	59.15	59.17
Level 1	50	59.15	59.20
Level 1	100	59.15	59.26
Level 2	20	59.14	59.31
Level 2	50	59.14	59.48
Level 2	100	59.13	59.61

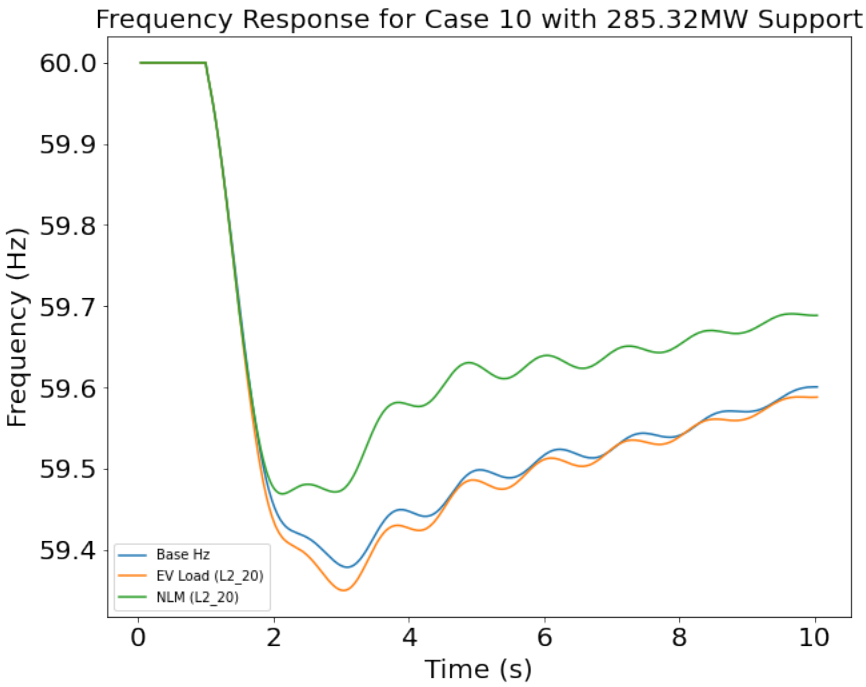

Figure 3.8: Comparison of Frequency Response using the 20 ports Level 2 charger of 7kW support per port on the base case, base case with just the positive EV load, and the base case with the Negative Load Model (NLM) on Case 10 with 131GWs.

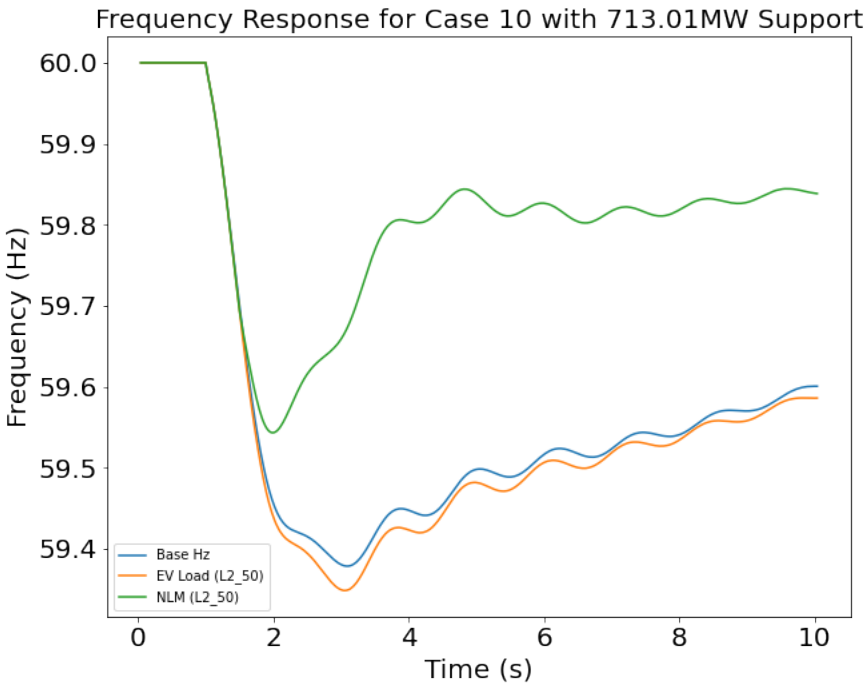

Figure 3.9: Comparison of Frequency Response using the 50 ports Level 2 charger of 7kW support per port on the base case, base case with just the positive EV load, and the base case with the Negative Load Model (NLM) on Case 10 with 131GWs.

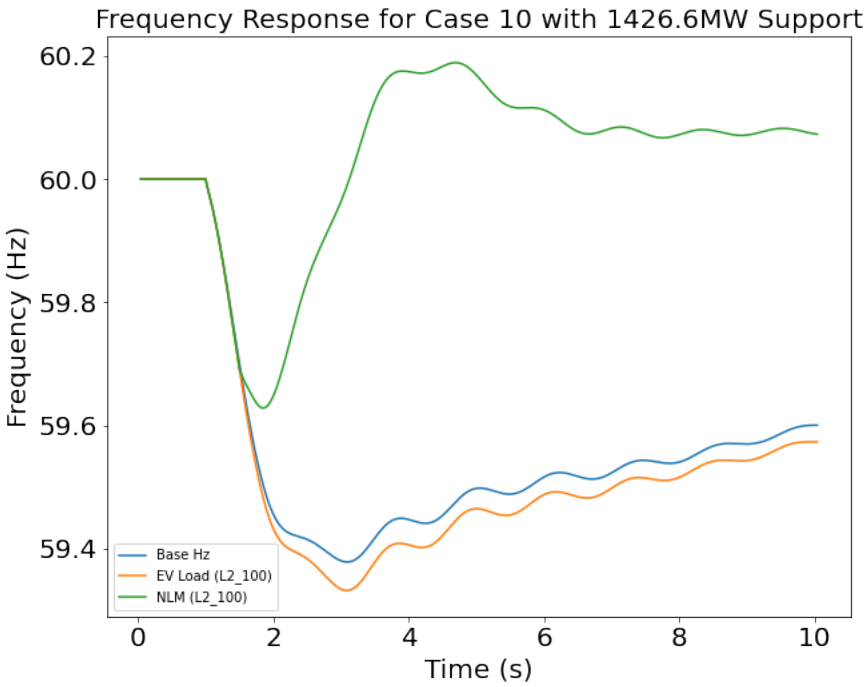

Figure 3.10: Comparison of Frequency Response using the 100 ports Level 2 charger of 7kW support per port on the base case, base case with just the positive EV load, and the base case with the Negative Load Model (NLM) on Case 10 with 131GWs.

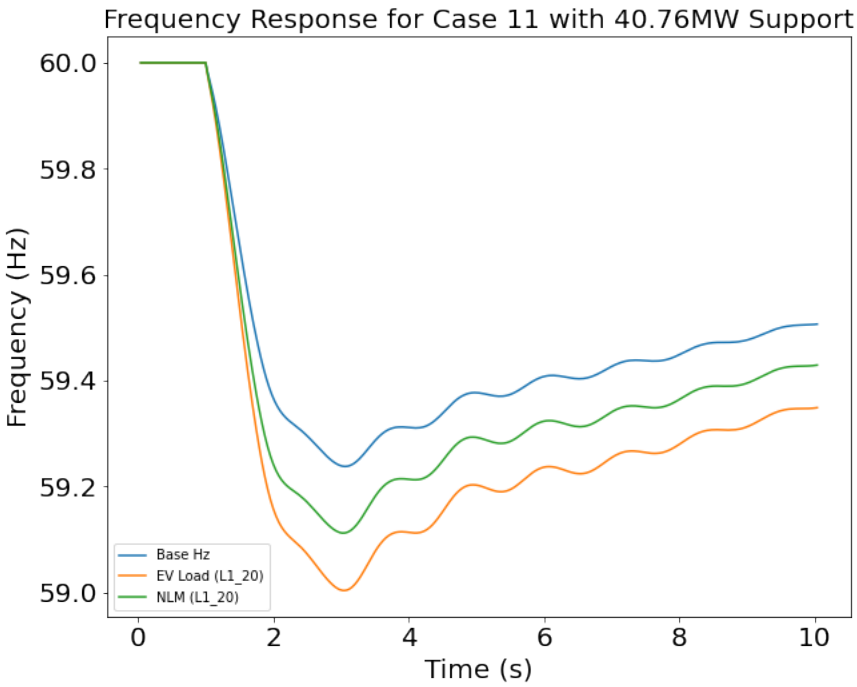

Figure 3.11: Comparison of Frequency Response using the 20 ports Level 1 charger of 1kW support per port on the base case, base case with just the positive EV load, and the base case with the Negative Load Model (NLM) on Case 11 with 116GWs.

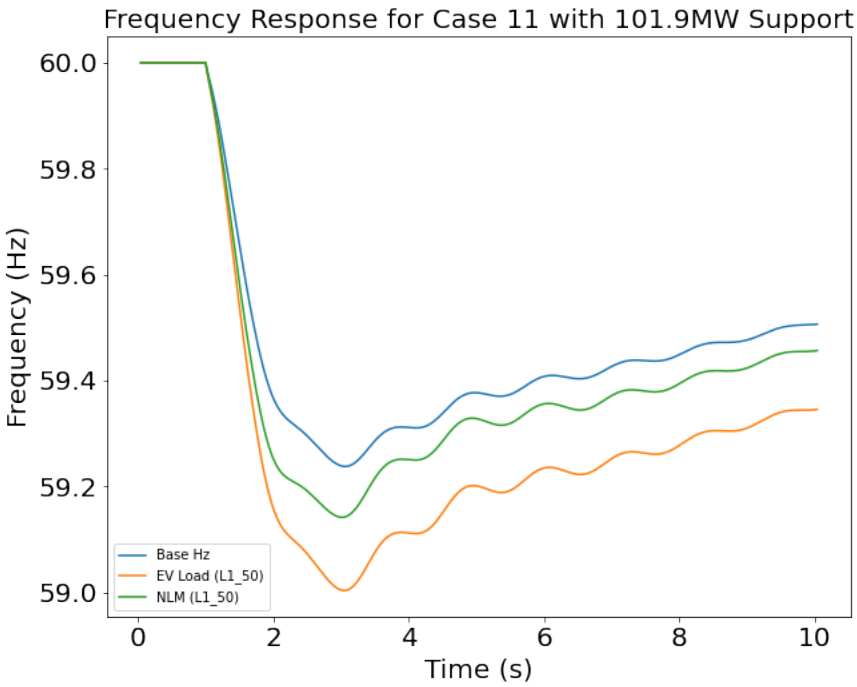

Figure 3.12: Comparison of Frequency Response using the 50 ports Level 1 charger of 1kW support per port on the base case, base case with just the positive EV load, and the base case with the Negative Load Model (NLM) on Case 11 with 116GWs.

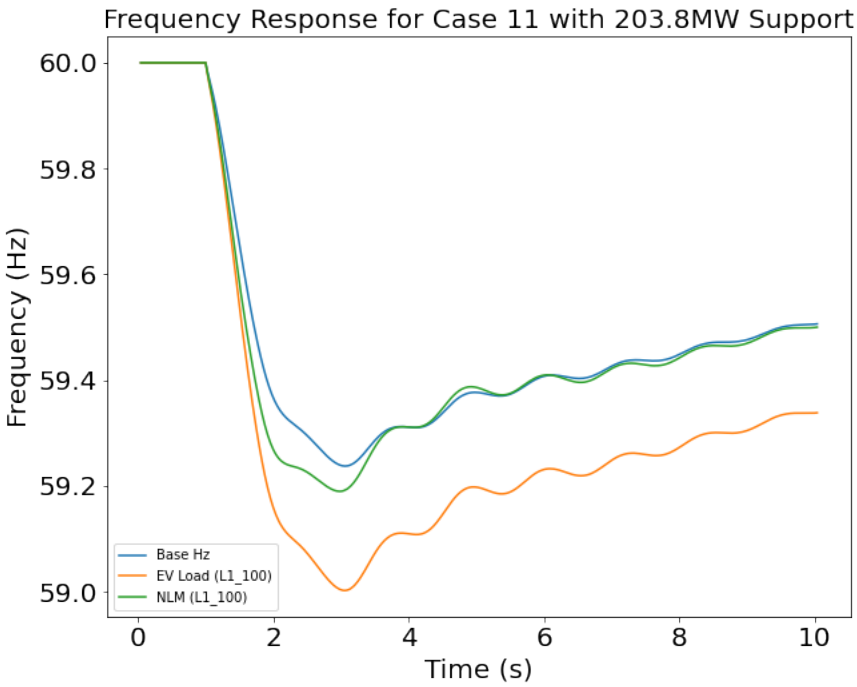

Figure 3.13: Comparison of Frequency Response using the 100 ports Level 1 charger of 1kW support per port on the base case, base case with just the positive EV load, and the base case with the Negative Load Model (NLM) on Case 11 with 116GWs.

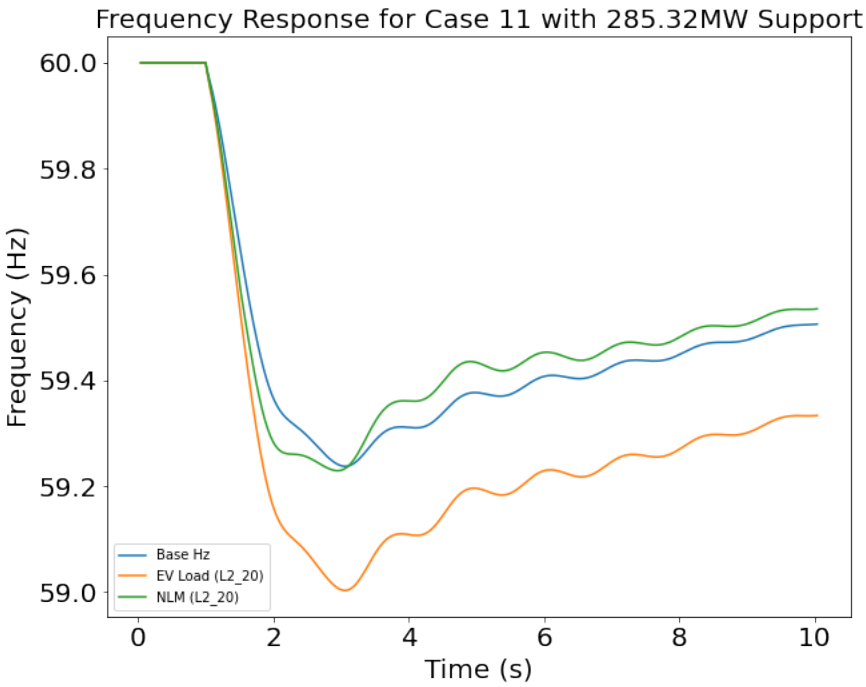

Figure 3.14: Comparison of Frequency Response using the 20 ports Level 2 charger of 7kW support per port on the base case, base case with just the positive EV load, and the base case with the Negative Load Model (NLM) on Case 11 with 116GWs.

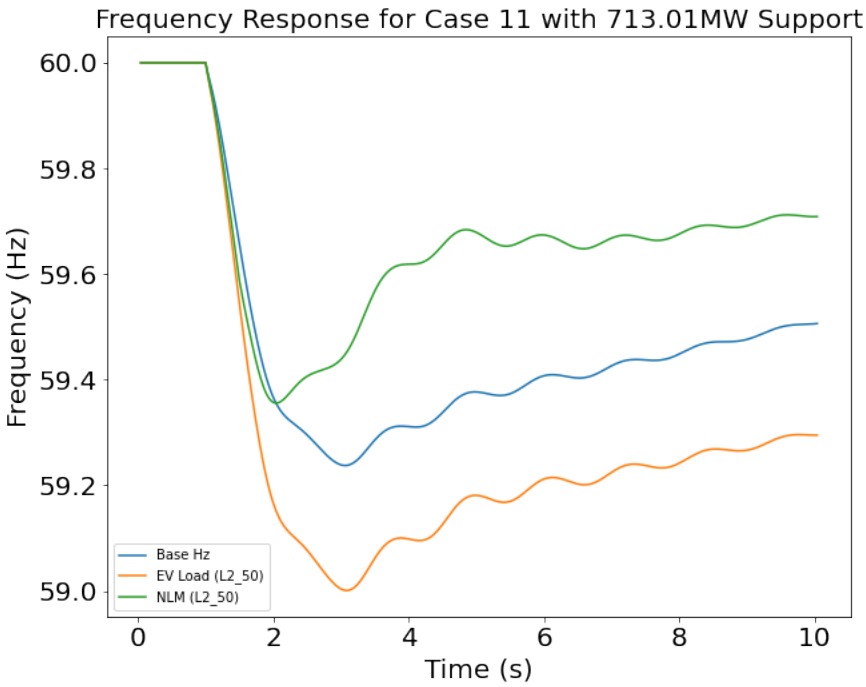

Figure 3.15: Comparison of Frequency Response using the 50 ports Level 2 charger of 7kW support per port on the base case, base case with just the positive EV load, and the base case with the Negative Load Model (NLM) on Case 11 with 116GWs.

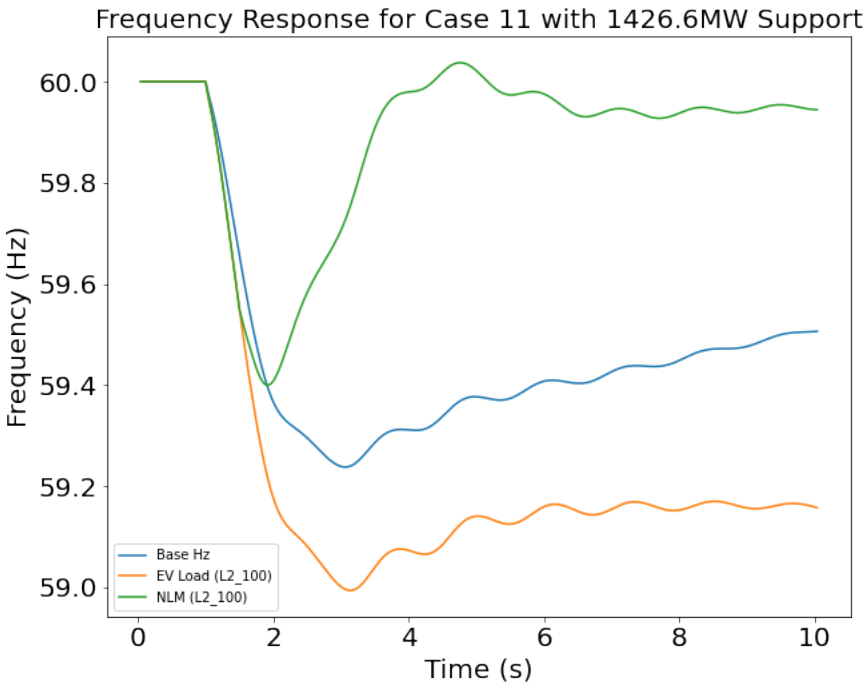

Figure 3.16: Comparison of Frequency Response using the 100 ports Level 2 charger of 7kW support per port on the base case, base case with just the positive EV load, and the base case with the Negative Load Model (NLM) on Case 11 with 116GWs.

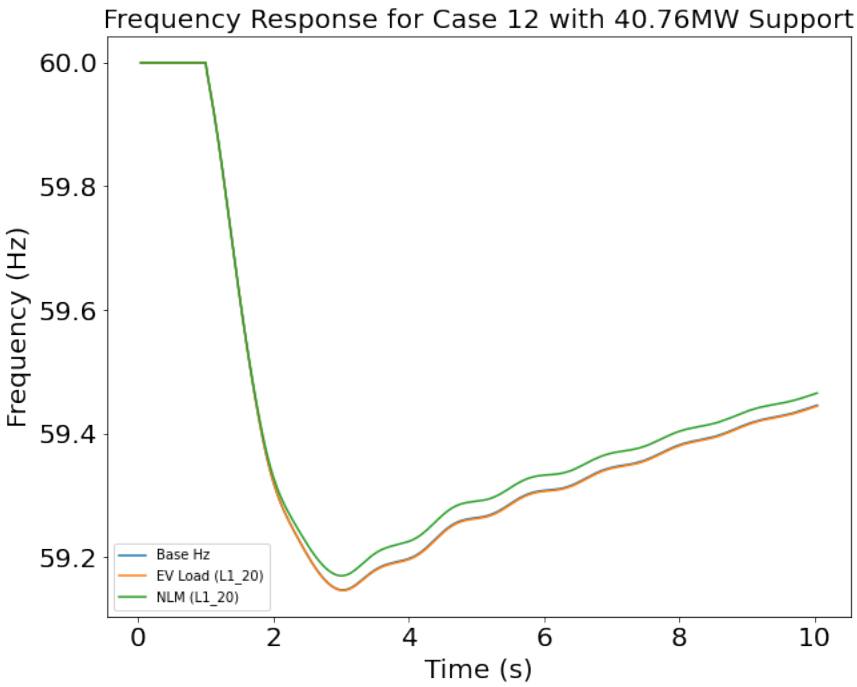

Figure 3.17: Comparison of Frequency Response using the 20 ports Level 1 charger of 1kW support per port on the base case, base case with just the positive EV load, and the base case with the Negative Load Model (NLM) on Case 12 with 100GWs.

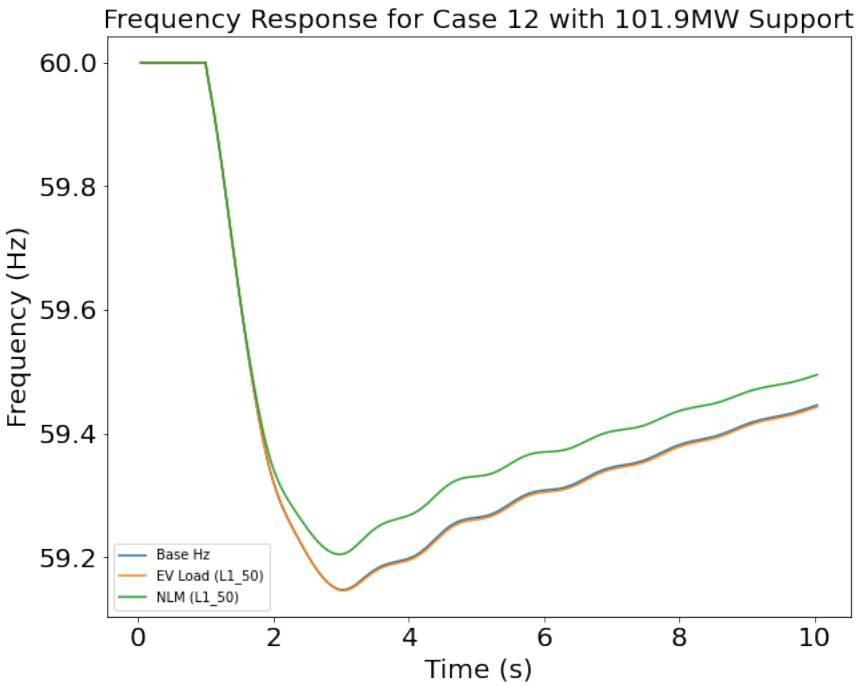

Figure 3.18: Comparison of Frequency Response using the 50 ports Level 1 charger of 1kW support per port on the base case, base case with just the positive EV load, and the base case with the Negative Load Model (NLM) on Case 12 with 100GWs.

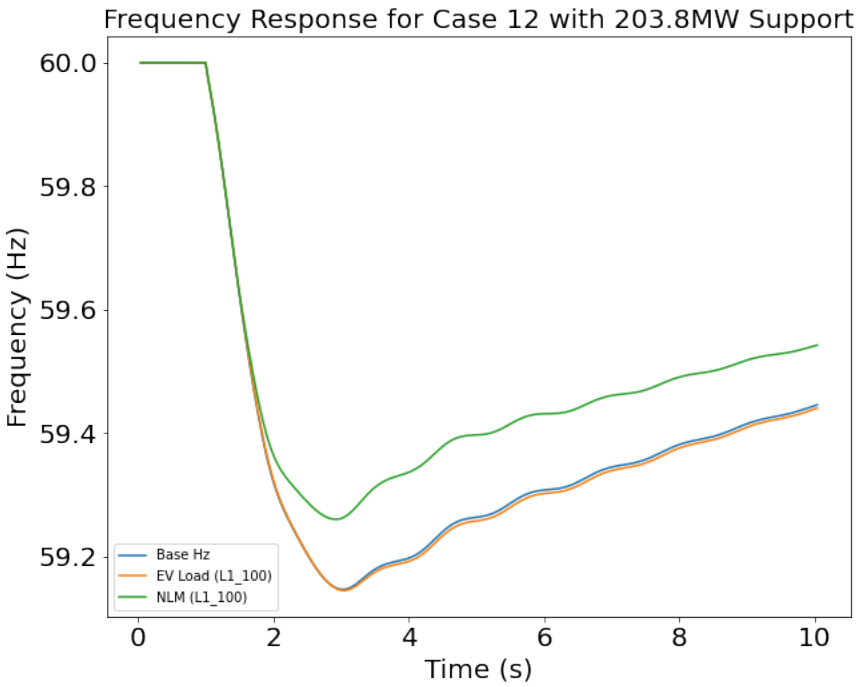

Figure 3.19: Comparison of Frequency Response using the 100 ports Level 1 charger of 1kW support per port on the base case, base case with just the positive EV load, and the base case with the Negative Load Model (NLM) on Case 12 with 100GWs.

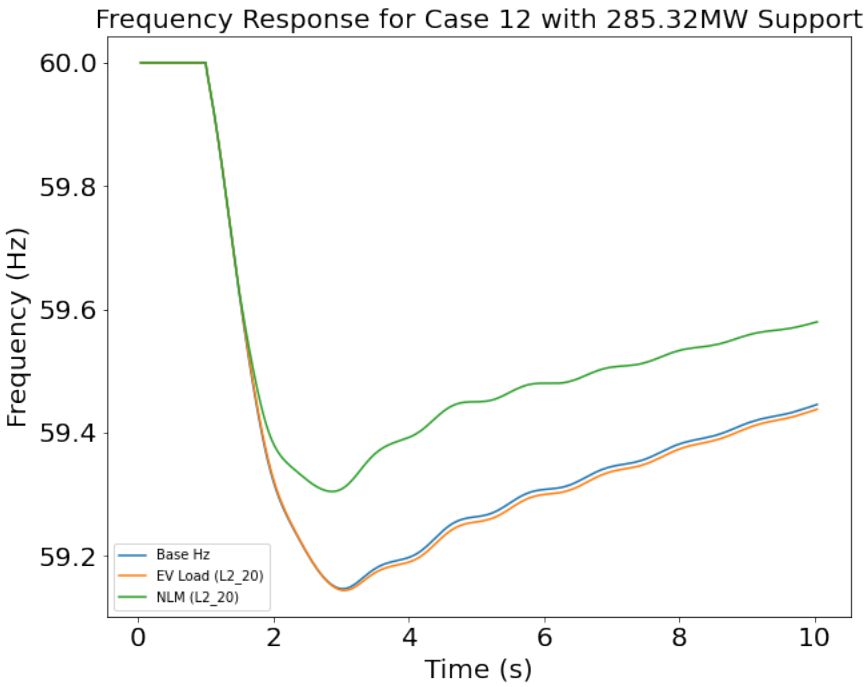

Figure 3.20: Comparison of Frequency Response using the 20 ports Level 2 charger of 7kW support per port on the base case, base case with just the positive EV load, and the base case with the Negative Load Model (NLM) on Case 12 with 100GWs.

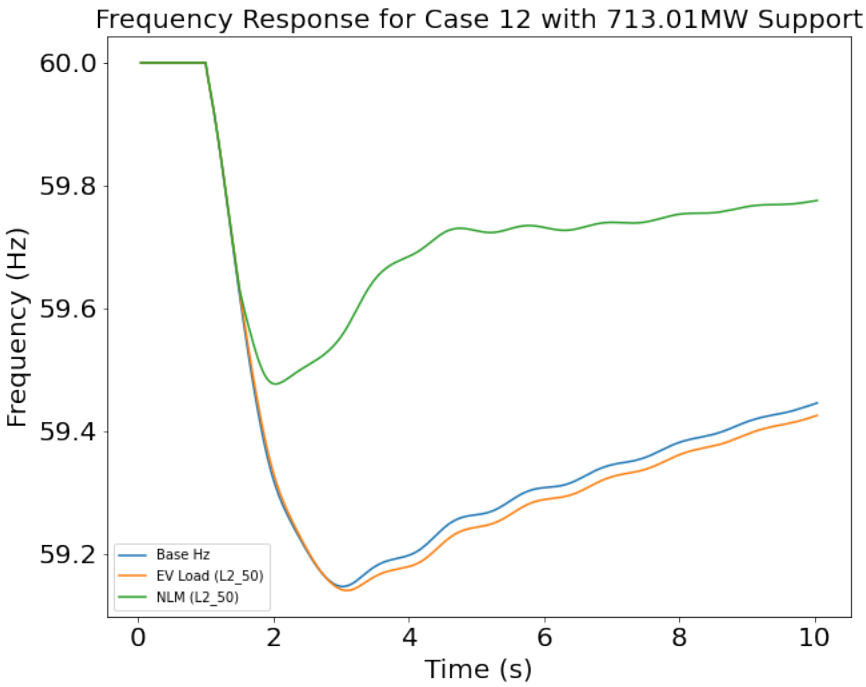

Figure 3.21: Comparison of Frequency Response using the 50 ports Level 2 charger of 7kW support per port on the base case, base case with just the positive EV load, and the base case with the Negative Load Model (NLM) on Case 12 with 100GWs.

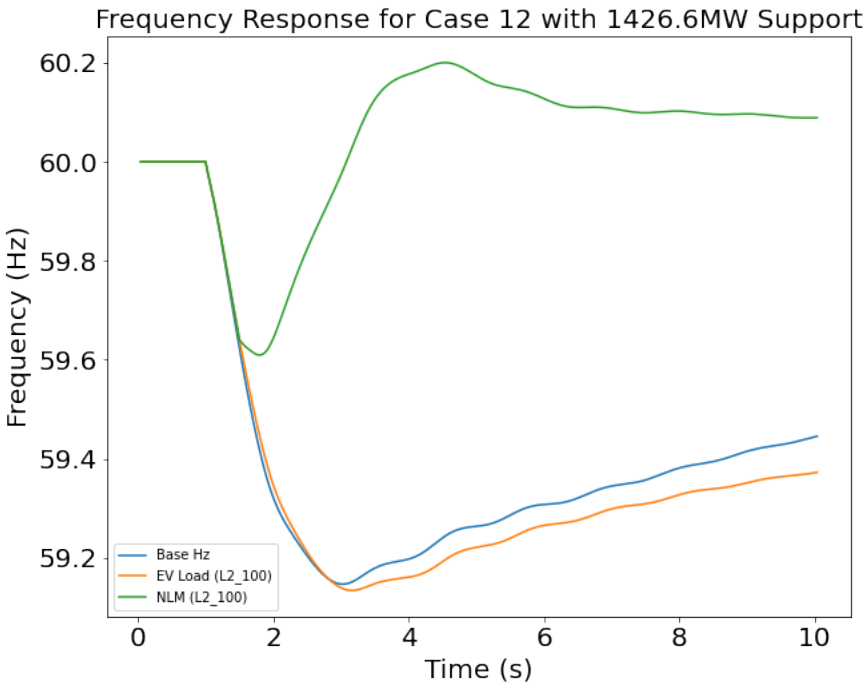

Figure 3.22: Comparison of Frequency Response using the 100 ports Level 2 charger of 7kW support per port on the base case, base case with just the positive EV load, and the base case with the Negative Load Model (NLM) on Case 12 with 100GWs.

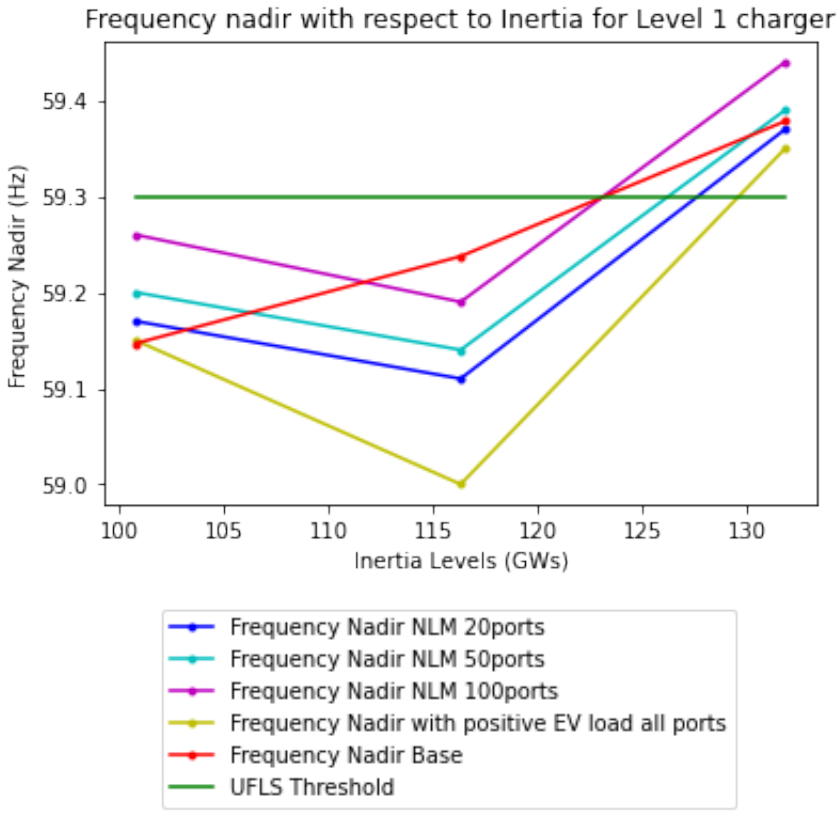

Figure 3.23: Frequency Nadir comparison of the base case, base case with positive EV load, and base case with NLM to the UFLS threshold for Level 1 charger.

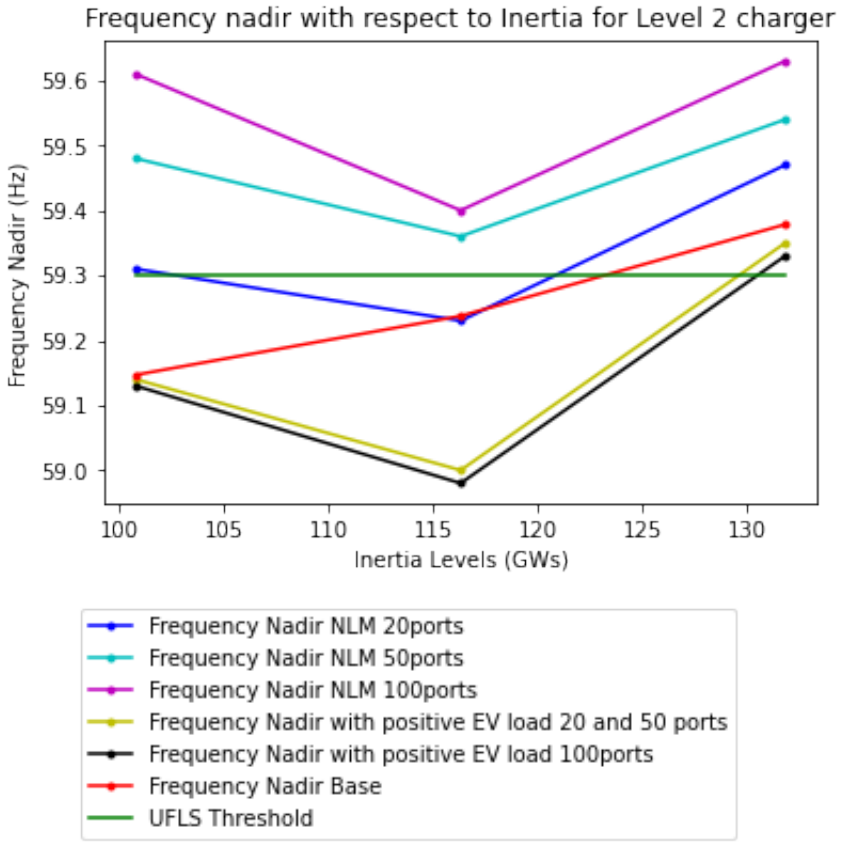

Figure 3.24: Frequency Nadir comparison of the base case, base case with positive EV load, and base case with NLM to the UFLS threshold for Level 2 charger.

4. SUMMARY AND CONCLUSIONS

This project evaluates the impact of renewable penetration on the inertia of the power system. It can be concluded that the increasing level of renewable sources penetration decreases the inertia and eventually the frequency response of the power system. This is expected to be a challenging problem for the future of the power grid as the renewable sources on the grid are projected to increase.

Analysis on the Texas 7k bus system under varying inertia are examined to evaluate the frequency response of the system. The result showed that for inertia levels of Case 11 and 12 which are 116 GWs and 100 GWs respectively, the frequency nadir is below the UFLS threshold frequency of 59.3 Hz. Including just the positive EV load on the system to represent the current trend shows that the frequency nadir of the system further decreases after the same contingency as in the base case. The utilization of EV fleets is proposed in this project as an ancillary service to provide inertia support to such cases during a disturbance like the outage of the largest generation unit. These EV fleets are modeled using a Negative Load Model which aggregates the demand from the EV charging station to the power grid simulation as positive loads at four Texas cities' buses, and aggregates the supply from the EV fleets as negative loads at the same cities' buses. The positive loads reflects a normal operation while the negative load reflects the contingency operation. The results are compared for the inertia cases with and without the Negative Load Model. The comparison of the results shows that the implementation of EV fleets for inertia support during a disturbance through the utilization of the Negative Load Model improves the RoCoF and frequency nadir of the system to a value that is above the Underfrequency load shed set points.This is important for avoiding an involuntary load shed on the system. Levels of EV fleets penetration were also analyzed to represent future EV trends and their impact on the frequency response of the power system, this proved to yield good results for the goal of this project.

4.1 Challenges

Deciding the model to use for the intended goal of the project was challenging.The difficulty in selecting the optimal model for a modeling study arises from a lack of clear comprehension about how the efficacy of the study hinges on the specific model employed. This made it difficult to establish a clear definition of model performance. Various available models that could be modified for the purpose of the project were reviewed before finally deciding on the model used. Although the WECC model seemed promising, only the Negative Load Model was implemented due to the time constraint. Some assumptions were made in the studies conducted for this project due to difficulties surrounding the acquisition of data of electric vehicles.

4.2 Further Study

For future work, an analysis of the U.S. Western Electricity Coordinating Council (WECC) battery models should be implemented for inertia frequency regulation of the Texas 7k bus system under varying inertia to further analyze in greater detail the impacts of EVs fleets on inertia response. This can be compared to the Negative Load Model for evaluation based on the metrics defined for model performance..

REFERENCES

[1] National Renewable Energy Laboratory, "Tutorial of wind turbine control for supporting grid frequency through active power control," tech. rep., National Renewable Energy Laboratory, 2012.

[2] ERCOT, "Inertia: Basic concepts and impacts on the ercot grid," *ERCOT : https://www.ercot.com/files/docs/2018/04/04/Inertia_Basic_Concepts_Impacts_On_ERCOT_v0.pdf*, 2018.

[3] X. Xu, M. Bishop, D. G. Oikarinen, and C. Hao, "Application and modeling of battery energy storage in power systems," *CSEE Journal of Power and Energy Systems*, vol. 2, no. 3, pp. 82–90, 2016.

[4] O. Oshinkoya, J.-O. Baek, J. Kao, and A. Birchfield, "Preliminary analysis of the potential impact of electric vehicle fleets on large power system inertia floor," in *2023 IEEE Texas Power and Energy Conference (TPEC)*, pp. 1–6, 2023.

[5] ChargeHub, "General ev charging information.," *ChargeHub : https://chargehub.com/en/countries/united-states/texas/katy.html*, 2022.

[6] U.S. Department of Energy, "Electricity production and distribution," *DOE : https://afdc.energy.gov/fuels/electricity_production.html#:~:text=According%20to%20the%20U.S.%20Energy,biomass%2C%20wind%2C%20and%20geothermal*, 2022.

[7] U.S. Energy Information Administration, "Today in energy," *EIA : https://www.eia.gov/todayinenergy/detail.php?id=51698#:~:text=In%20our%20Annual%20Energy%20Outlook,new%20wind%20and%20solar%20power*, 2022.

[8] National Renewable Energy Laboratory, "Inertia and the power grid: A guide without the spin," tech. rep., National Renewable Energy Laboratory, 2020.

[9] A. Bera, M. Abdelmalak, S. Alzahrani, M. Benidris, and J. Mitra, "Sizing of energy storage systems for grid inertial response," in *2020 IEEE Power & Energy Society General Meeting (PESGM)*, pp. 1–5, 2020.

[10] R. Evode, "Modeling of electric grid behaviors having electric vehicle charging stations with g2v and v2g possibilities," in *2021 International Conference on Electrical, Computer, Communications and Mechatronics Engineering (ICECCME)*, pp. 1–5, 2021.

[11] J. Hu, H. Morais, T. Sousa, and M. Lind, "Electric vehicle fleet management in smart grids: A review of services, optimization and control aspects," *Renewable and Sustainable Energy Reviews*, vol. 56, pp. 1207–1226, 04 2016.

[12] K. S. Ratnam, K. Palanisamy, and G. Yang, "Future low-inertia power systems: Requirements, issues, and solutions - a review," *Renewable and Sustainable Energy Reviews*, vol. 124, p. 109773, 2020.

[13] H. T. Nguyen, G. Yang, A. H. Nielsen, and P. H. Jensen, "Frequency stability improvement of low inertia systems using synchronous condensers," in *2016 IEEE International Conference on Smart Grid Communications (SmartGridComm)*, pp. 650–655, 2016.

[14] Nahid-Al-Masood, N. Modi, and R. Yan, "Low inertia power systems: Frequency response challenges and a possible solution," in *2016 Australasian Universities Power Engineering Conference (AUPEC)*, pp. 1–6, 2016.

[15] M. Krpan and I. Kuzle, "Impact of ultracapacitor modelling on fast frequency control performance," in *2020 International Conference on Smart Grids and Energy Systems (SGES)*, pp. 326–331, 2020.

[16] A. Berizzi, A. Bolzoni, A. Bosisio, V. Ilea, D. Marchesini, R. Perini, and A. Vicario, "Synthetic inertia from wind turbines for large system stability," in *2020 IEEE International Con-*

ference on Environment and Electrical Engineering and 2020 IEEE Industrial and Commercial Power Systems Europe (EEEIC / I&CPS Europe), pp. 1–6, 2020.

[17] A. Dubey and S. Santoso, "Electric vehicle charging on residential distribution systems: Impacts and mitigations," *IEEE Access*, vol. 3, pp. 1871–1893, 2015.

[18] Edison Electric Institute, "Eei projects 26.4 million electric vehicles will be on u.s. roads in 2030," *EEI : https://www.eei.org/News/news/All/eei-projects-26-million-electric-vehicles-will-be-on-us-roads-in-2030*, 2022.

[19] K. W. and L. S., "Electric vehicles as a new power source for electric utilities," *Transportation Research Part D: Transport and Environment*, vol. 2, no. 3, pp. 157–175, 1997.

[20] Y. Zhou and X. Li, "Vehicle to grid technology: A review," in *2015 34th Chinese Control Conference (CCC)*, pp. 9031–9036, 2015.

[21] E.ON Energy, "Electric car battery capacity lifespan," *EON : https://www.eonenergy.com/electric-vehicle-charging/costs-and-benefits/battery-capacity-and-lifespan.html#:~:text=Electric%20car%20battery%20capacity,-Lithium%2Dion%20battery&text=The%20average%20capacity%20is%20around,higher%20the%20kWh%20the%20better.*, 2022.

[22] Texas A&M Transportation Institute, "Electric vehicle (ev) dashboard," *TTI: https://txaqportal.org/analytics*, 2022.

[23] U.S. Environmental Protection Agency, "Biden-harris administration will double clean school bus rebate awards to nearly $1 billion.," 2022.

[24] A. B. Birchfield, T. Xu, K. M. Gegner, K. S. Shetye, and T. J. Overbye, "Grid structural characteristics as validation criteria for synthetic networks," *IEEE Transactions on Power Systems*, vol. 32, no. 4, pp. 3258–3265, 2017.

[25] Texas AM University, "Electric grid test case repository," *TAMU : https://electricgrids.engr.tamu.edu/*, 2022.

[26] Z. Zhou, W. Wang, T. Lan, and G. M. Huang, "Dynamic performance evaluation of grid-following and grid-forming inverters for frequency support in low inertia transmission grids," in *2021 IEEE PES Innovative Smart Grid Technologies Europe (ISGT Europe)*, pp. 01–05, 2021.

[27] European Network of Transmission System Operators for Electricity, "Inertia and Rate of Change of Frequency (RoCoF)," 2022. 2022-12-5.

[28] Federal Energy Regulatory Commission, "Automatic underfrequency load shedding and load shedding plans reliability standards," 2011.

[29] North American Electric Reliability Corporation, "Response to ferc supplemental request for information on the status of underfrequency load shedding," 2008.

[30] Electricity Reliability Council of Texas, "Nprr 1128 on ffr procurement," *ERCOT : https://www.ercot.com/files/docs/2022/05/19/NPRR_1128_WMWG_Discussion_v1.pptx*, 2022.